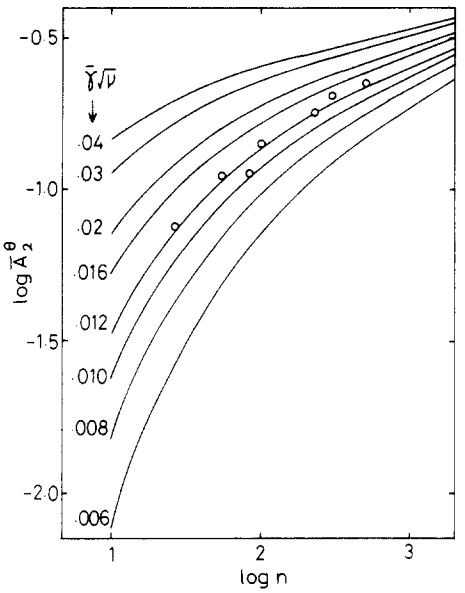

Figure 2. log-log plot of reduced topological second virial coefficient, $\bar{A}_2^{\Theta}$ vs. n. Numbers attached to curves represent $\bar{\gamma}\nu^{1/2}$. Open circles are experimental data of Roovers and Toporowski for polystyrene in cyclohexane at 35 °C;[1] they are fitted to the theoretical curve for $\bar{\gamma}\nu^{1/2} = 0.012$.

Results and Discussion. It is convenient to introduce a reduced second virial coefficient, $\bar{A}_2^{\Theta} = (2M^{1/2}M_0^{3/2}/N_A\bar{b}^3)A_2^{\Theta}$, which is a function of n and $\bar{\gamma}\nu^{1/2}$ alone; here M_0 is the molecular weight of the repeat units. Calculation of A_2^{Θ} is done in almost the same way as in TDFRP-I: A_2^{Θ} is defined by eq 1, and $P_0(\mathbf{w})$, G^{I}, and G^{II} are given by eq 4.19b.I, 4.9.I, 4.10a,I, and 4.10b.I; the only difference is in the calculation of the contact probabilities for submolecules, $P(0_{00}|\mathbf{w})$ and $P(0_{ij}|0_{00},\mathbf{w})$ which is done by using exact expressions for finite n instead of using the approximate eq 4.7a.I and 4.7b.I (which are exact only for $n \to \infty$). Results of calculation[9] are shown in Figure 2, in which log $\bar{A}_2^{\Theta}$ is plotted against log n for various $\bar{\gamma}\nu^{1/2}$. In plotting experimental data in Figure 2, the ordinate (log $\bar{A}_2^{\Theta}$) is determined uniquely but the abscissa (log n) is uncertain by an amount log ν. The Roovers-Toporowski data for PS agree well with theoretical curves for $0.008 \leq \bar{\gamma}\nu^{1/2} \leq 0.020$ ($\bar{b} = 0.72_0$ nm is assumed). This leads to $3.72 \leq \nu \leq 23.4$ and $\bar{\gamma} = 0.0041_4$. As an example, data for $\nu = 8.51$ are shown in Figure 2 by open circles, which are in good agreement with a theoretical curve for $\bar{\gamma}\nu^{1/2} = 0.012$. It is important here that (1) the same $\bar{\gamma}$ (=0.0041) is obtained for $3.72 \leq \nu \leq 23.4$ (2) conditions (4) are roughly satisfied by this ν. It is interesting to compare this result with that of the 6-choice SCLMP,[2] of which bond vectors are in effect connected by free joints and which may therefore be considered as a standard model polymer: comparison of $\bar{\gamma}$ of these polymers shows that one free jointed bond (of the 6-choice SCLMP) corresponds to 3.4_6 (=$(0.0495/0.0041_4)^{1/2}$) repeat units of PS, a results which seems reasonable considering that bond angles are fixed and bulky side groups are attached to the main chain of PS. In rubber-elasticity, typical polymers are not PS but polyisoprene, polybutadiene, or poly(dimethylsiloxane), but their $\bar{\gamma}$ are not known at present because there are no data for their A_2^{Θ}. Ring poly(dimethylsiloxane) has been already synthesized and A_2 has been measured in good solvents but, unfortunately, A_2^{Θ} has not.[10] It is expected that A_2^{Θ} of many other polymers will be measured in the future.

Registry No. PS (homopolymer), 9003-53-6.

References and Notes

(1) Roovers, J.; Toporowski, P. M. *Macromolecules* **1983**, *16*, 843.
(2) Iwata, K.; Kimura, T. *J. Chem. Phys.* **1981**, *74*, 2039.
(3) Iwata, K. *J. Chem. Phys.* **1983**, *78*, 2778.
(4) The topological problem of ring polymers had also been discussed in the following papers: Brereton, M. G.; Sharh, S. *J. Phys. A: Math. Gen.* **1981**, *14*, 51; des Cloizeaux, J. *J. Phys. (Paris), Lett.* **1981**, *42*, 433; Tanaka, F. *Prog. Theor. Phys.* **1982**, *68*, 164.
(5) Iwata, K. *J. Chem. Phys.* **1982**, *76*, 6363, 6375.
(6) See, for example: Gottlieb, M., et al. *Macromolecules* **1981**, *14*, 1039.
(7) Iwata, K. *J. Chem. Phys.* **1980**, *73*, 562.
(8) Equations of TDFRP-I are indicated by attaching the symbol .I to the equation numbers.
(9) A detailed numerical table of $\bar{A}_2^{\Theta}$ is available from the author on request.
(10) Edwards, C. J. C.; Stepto, R. F. T.; Semlyen, J. A. *Polymer* **1982**, *23*, 869.

Kazuyoshi Iwata
The Research Institute for Material Science and Engineering, Fukui University
Bunkyo 3, Fukui 910, Japan

Received July 9, 1984

Phase Separation in Polyurethanes—A Deuterium NMR Study

Although numerous models have been set forth concerning the morphological microdomain structure for polyurethanes,[1] there is at present no consensus in this matter. Bonart et al.,[2-5] on the basis of wide-angle X-ray scattering (WAXS) and small-angle X-ray scattering (SAXS) experiments, have proposed hard segment packing models in which the hard segments assume fully extended configurations within lamellar or sheetlike domains. This model is represented schematically in Figure 1a. Subsequent WAXS studies by Blackwell et al.[6] supported this model.

However, recent results by Van Bogart et al.[7] and Koberstein and Stein[8] are inconsistent with an extended sequence model. Using SAXS, both groups of investigators find that the hard segment chains must be present in either coiled or perhaps folded configurations. Koberstein and Stein developed a new model based on these results.[8] In this model, the hard segment domain thickness is governed predominantly by the shortest hard segment sequence length that is insoluble in the soft segment phase. Sequences longer than this critical length adopt coiled configurations to reenter the hard segment domain and fill space efficiently. Further detailed SAXS experiments on a series of polyurethanes of varying hard segment content support this model.[1] The Koberstein-Stein model is represented schematically in Figure 1b.

In this communication we present data that further define the nature of phase separation and hard-segment phase mixing in polyurethanes. In particular, our results address the following questions: (1) What fraction of the hard segment has motional characteristics identical to the pure hard segment material? (2) How does this fraction change as a function of the weight percent of hard component? and (3) How do the deuterium NMR data compare with the results of SAXS?

We have shown previously that solid-state deuterium NMR spectroscopy[9-12] is an exceptionally powerful tool for addressing the molecular details of phase separation in segmented copolyesters.[13,14] Deuterium NMR discriminates on the basis of molecular motion between those hard segments that are identical with the pure hard segment

0024-9297/85/2218-0116$01.50/0

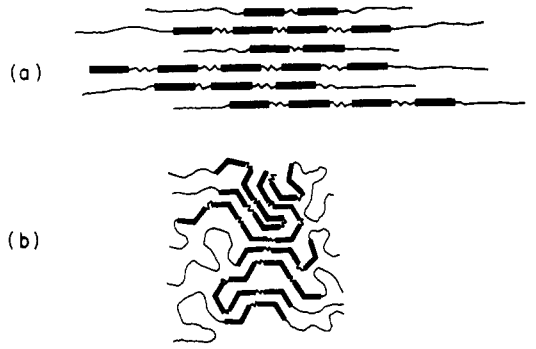

Figure 1. Schematic representation of (a) the extended hard segment configuration model, and (b) the Koberstein–Stein model.[8] The bars represent the MDI units.

material and those that are "dissolved" in the soft segment phase. Here we apply solid-state quadrupole echo deuterium NMR spectroscopy to the specifically labeled polyurethanes containing 100, 70, 60, and 50 % hard segment. The polymers were prepared in solution by standard techniques[15,16] and contain hard and soft blocks represented schematically as follows:

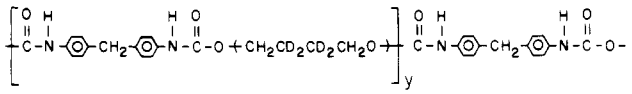

HARD SEGMENT

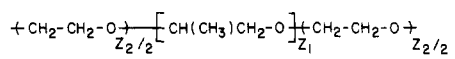

SOFT SEGMENT

Because the polymers are labeled specifically at the butanediol moiety of the hard segment, the deuterium NMR spectra reflect the motional environment of this group only, and do not contain contributions from the 4,4′-methylenebis(phenyl isocyanate) (MDI) or the soft segment polyol residues.

The deuterium NMR spectra[19] for these four samples are shown in Figure 2. The middle column (Figure 2d–f) shows the spectrum obtained at 22 °C of the all-hard segment material at different vertical scales. This spectrum, although ca. 120 kHz in breadth, is clearly not that of a Pake doublet.[25] Instead, it is reminiscent of the spectra observed for similarly labeled poly(butylene terephthalate), in which gauche–trans conformational jumps occur at an intermediate rate on the NMR time scale.[20] Spin–lattice relaxation experiments show that the T_1 of this component is ca. 20 ms. Experiments performed with very long recycle delays indicate that more than 90% of the sample contributes signal intensity to this spectrum. Temperature-dependent experiments are under way to further define the exact details of the molecular motion of the butanediol group in this material.

The spectra shown in Figure 2a–c correspond to the polyurethane samples containing 70, 60, and 50 wt % hard segments, respectively. In addition to the broad, 120 kHz pattern, these spectra also show a sharp line. That the spectra shown in Figure 2a–c are composed of two components can be shown from inversion–recovery spectra, in which the broad and the sharp components are observed to invert at different delay times. (Detailed solid- and solution-state relaxation experiments are under way and will be reported later.) The broad component is attributed to those hard segments that reflect molecular motion which is identical with that of the all-hard segment material. These hard segments would constitute the core of the hard

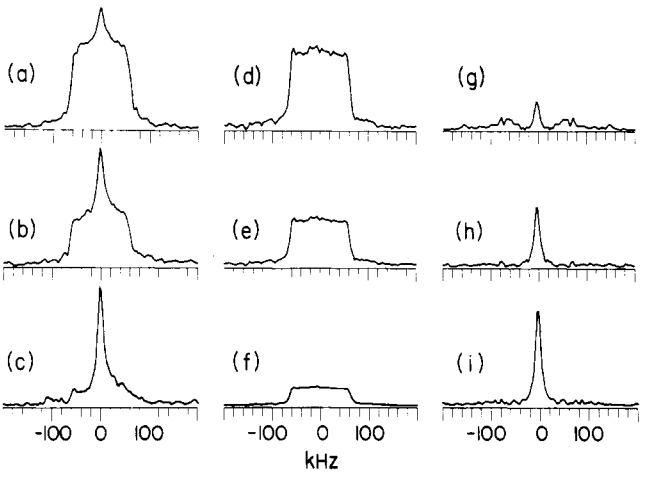

Figure 2. Solid-state quadrupole echo deuterium NMR spectra of hard segment labeled polyurethanes obtained at 22 °C and 55.26 MHz. Spectrum (a) 70, (b) 60, and (c) 50 wt % hard segment. Spectra d–f are of the all-hard segment material reported at different vertical gains. Spectra g–i were obtained by subtracting an appropriate amount of the symmetrized spectra in the center column from those in the left column. All spectra were obtained with a 2-s recycle delay.

segment-rich microdomains. The sharp component indicates the occurrence of molecular motions that are nearly isotropic in nature and may be associated with hard segments residing in a more mobile environment. Such increased mobility would be expected for hard segment sequences that are short enough to dissolve in the soft segment-rich microdomains but may also be found for hard segments that reside in the diffuse boundary region between the hard and soft segment microdomains.

The difference spectra shown in Figure 2g–i were obtained by subtracting the spectra in Figure 2d–f from those in Figure 2a–c. It is interesting to note that the line widths of these sharp components are identical; i.e., they are not a function of the hard segment content of the polymer. The fraction of sharp component can be estimated by appropriate integration of these spectra.[26] These fractions are listed in Table I and can be compared to SAXS estimates[27] of dissolved hard segment content.

The SAXS estimates are determined by assuming that all hard segment sequences of length equal to or less than a critical length, N_c, are dissolved in the soft segment phase. The critical segment length is determined from the experimental value of the hard segment domain thickness T_{HS} (see Table I). For the samples examined this length is equivalent to a hard segment containing approximately three MDI and two butanediol residues (i.e., $N_c \simeq 3$). The weight fraction of butanediol residues that are dissolved in the soft segment phase, ω_D, is then given by

$$\omega_D = \frac{\sum_{i=1}^{N_c} f_i(i-1)}{\bar{N}_n - 1}$$

where f_i is the number fraction of sequences containing $(i-1)$ butanediol residues calculated from Peebles' distribution function,[31] and $\bar{N}_n$ is the number average of MDI residues per hard segment sequence. The values of ω_D calculated in this fashion (Table I) are much smaller than the weight fraction of isotropic component estimated from the NMR measurements.

The weight fraction of butanediol residues residing in the interfacial gradient, ω_I, may also be determined from the SAXS results. If E is the width of a linear diffuse

Table I
Butanediol Hard Segment Component

overall wt % hard segment	hard domain thickness T_{HS}, nm	interphase width E, nm	% dissolved butanediol $\omega_D \times 100\%$	% butanediol in interfacial hard segment $\omega_I \times 100\%$	% dissolved and interfacial butanediol	% sharp butanediol component by NMR
70	7.7	1.1	2.1	13.5	15.6	14
60	7.3	1.1	4.0	14.4	18.4	20
50	6.1	1.1	7.8	15.9	23.7	50

boundary gradient between microdomains,[1,27] it is easily shown that $\omega_I = (R/T_{HS})(1 - \omega_D)$. Values for this quantity as well as for the weight percent of total dissolved and interfacial hard segment are presented in Table I. The total weight fractions of dissolved and interfacial hard segment estimated by the SAXS analyses are in good agreement with the NMR weight percents of isotropic component except for the sample containing 50 wt % hard segments, for which the NMR value is much higher. This discrepancy may arise from differences in the synthesis and molding procedures adopted for the NMR and SAXS samples.[15,27] SAXS experiments on the labeled NMR samples are currently in progress. It is apparent that hard segments residing in both the soft segment phase and within the interfacial gradient contribute to the sharp component observed in the NMR spectra. The NMR results provide support to, but do not prove, the validity of the Koberstein–Stein model.

The solid-state deuterium NMR results show that this interfacial area has very nearly isotropic motion on a 10^7 s^{-1} time scale. Such rapid, nearly isotropic motions are observed in flexible polymers such *cis*-polybutadiene and poly(dimethylsiloxanes). The rapid, nearly isotropic motions observed for these butanediol residues suggest that there are few long-lived *inter*urethane hydrogen-bonding interactions in this interfacial area.

It is appropriate to compare the quadrupole echo deuterium NMR results reported here with other NMR results.[32-38] Although they have not been performed on identical polyurethanes, the overall conclusions are relevant to the system at hand.

Using broadline proton NMR, Assink[32,33] finds two components. One decays rapidly and is attributed to the MDI hard segments, whereas the other decays more slowly and is assigned to the polyester soft segments. With proton spin diffusion as an experimental probe, Assink and Wilkes[34,35] evaluated phase mixing in a series of MDI–polyester polyurethanes. Their data require the presence of both short- and long-range degrees of mixing. The short-range mixing is attributed to distances involving several molecular diameters, whereas the long-range mixing is attributed to chain entanglement effects. Their results point to a fair fraction of interfacial material.

The deuterium NMR experiments reported in this work substantiate and expand on the results of Assink and Wilkes. Because only the hard segment is labeled in the present case, all ambiquities concerning the source of the signal (i.e., hard or soft segments) are removed. Furthermore, deuterium NMR spectra are dominated by quadrupolar relaxation, and spin diffusion is not a factor in interpreting the data. Most importantly, the material comprising the interfacial area can now be directly examined and quantified by NMR measurements.

The results reported in this communication show that the solid-state deuterium NMR experiment holds much promise for providing rich and detailed information concerning microphase separation in polyurethanes and other phase-separated polymers. Multiple experiments along the lines described here are in progress and will be described at a later date.

Acknowledgment. The part of this work performed at Princeton was supported in part by the Office of Naval Research.

Registry No. (MDI)·(1,4-butanediol) (copolymer), 25805-16-7; (MDI)·(1,4-butanediol)·(polyethylene glycol)·(polypropylene glycol) (copolymer), 76701-49-0.

References and Notes

(1) For a review of current work in this area, see: Leung, L. M.; Koberstein, J. T. *J. Polym. Chem., Polym. Phys. Ed.*, in press.
(2) Bonart, R.; Morbitzer, L.; Hentze, G. *J. Macromol. Sci., Phys.* **1969**, *B3*, 337.
(3) Bonart, R.; Morbitzer, L.; Muller, E. H. *J. Macromol. Sci., Phys.* **1974**, *B9*, 447.
(4) Bonart, R.; Muller, E. H. *J. Macromol. Sci., Phys.* **1974**, *B10*, 177.
(5) Bonart, R.; Muller, E. H. *J. Macromol. Sci., Phys.* **1974**, *B10*, 345.
(6) Blackwell, J.; Lee, C. D. *J. Polym. Sci., Polym. Phys. Ed.* **1983**, *21*, 2169 and references cited.
(7) Van Bogart, J. W. C.; Gibson, P. E.; Cooper, S. L. *J. Polym. Sci., Polym. Phys. Ed.* **1983**, *21*, 65.
(8) Koberstein, J. T.; Stein, R. S. *J. Polym. Sci., Polym. Phys. Ed.* **1983**, *21*, 1439.
(9) Jelinski, L. W. In "High Resolution NMR of Synthetic Polymers in Bulk"; Komoroski, R. A., Ed.; Verlag Chemie: Weinheim, 1985.
(10) Spiess, H. W. *Colloid Polym. Sci.* **1984**, *261*, 193.
(11) Spiess, H. W. *J. Mol. Struct.* **1983**, *111*, 119.
(12) Spiess, H. W. In "Advances in Polymer Science"; Kausch, H. H., Zachmann, H. G., Eds.; Springer-Verlag: Berlin, 1984.
(13) Jelinski, L. W.; Dumais, J. J.; Engel, A. K. *ACS Symp. Ser.* **1984**, *No. 247*, 55.
(14) Jelinski, L. W.; Dumais, J. J.; Engel, A. K. *Org. Coat. Appl. Polym. Sci. Proc.* **1983**, *248*, 102.
(15) The polyurethanes used in this study were synthesized in THF solution under a dry argon atmosphere following established literature procedures (see, for example: ref 16). The hard segment is 4,4′-methylenebis(phenyl isocyanate) (MDI) (Eastman Kodak) chain extended with butanediol-2,2,3,3-d_4 (Merck Isotopes). The soft segment is polyoxypropylene end-capped with 30.4 wt % oxyethylene (Union Carbide NIAX polyol, M_n = 2000, functionality = 1.94). NMR samples were cut from 2-mm thick disks that were molded under vacuum for ca. 5 min at 180–190 °C and 4000 psi and slow-cooled under pressure. Transurethanefication, known to be rapid above 170 °C,[17,18] should lead to a most probable distribution of sequence lengths.
(16) Lyman, D. J. *J. Polym. Sci.* **1960**, *45*, 49.
(17) Camberlin, Y.; Pascault, J. P.; Letoffe, M.; Claudy, P. *J. Polym. Sci., Polym. Chem. Ed.* **1982**, *20*, 383.
(18) Chang, A. L.; Briber, R. M.; Thomas, E. L.; Zdrahala, R. J.; Critchfield, F. E. *Polymer* **1982**, *23*, 1060.
(19) Solid-state deuterium NMR spectra were obtained on ca. 100-mg samples at 55.26 MHz for ^2H using a home-built spectrometer.[20] The quadrupole echo[21-23] and the inversion–recovery quadrupole echo pulse sequence[24] were used to observe the spectra. Detection was performed in quadrature by using 2K points per channel and a 100 ns/point (10 MHz) digitization rate. The 90° pulse width was 3.3 μs and the echo delay was 30 μs.
(20) Jelinski, L. W.; Dumais, J. J.; Engel, A. K. *Macromolecules* **1983**, *16*, 492.
(21) Davis, J. H.; Jeffrey, K. R.; Bloom, M.; Valic, M. I.; Higgs, T. P. *Chem. Phys. Lett.* **1976**, *42*, 390.
(22) Blinc, R.; Rutar, V.; Seliger, J.; Slak, J.; Smolej, V. *Chem. Phys. Lett.* **1977**, *48*, 576.
(23) Hentschel, R.; Spiess, H. W. *J. Magn. Reson.* **1979**, *35*, 157.
(24) Cholli, A. L.; Dumais, J. J.; Engel, A. K.; Jelinski, L. W. *Macromolecules* **1984**, *17*, 2399.
(25) Pake, G. E. *J. Chem. Phys.* **1948**, *16*, 327.
(26) These spectra have not been corrected for T_2 losses. Because

polymers are generally characterized by a distribution of motional frequencies, this assumption is expected to have a small effect on the reported integrals.[39]
(27) SAXS measurements of lamellar thickness and diffuse phase boundary thickness were carried out by analyses described in previous communications.[1,8] For the present study, bulk polymerized samples prepared from unlabeled butanediol[28] were employed in the SAXS studies. The samples were molded under vacuum at 180 °C and 4000 psi and slow cooled under pressure. The urethane exchange reaction is rapid at this temperature[17,18] and should correct for any nonrandom sequence length distribution which may have resulted during polymerization.[29,30]
(28) Zdrahala, R. J.; Critchfield, F. E.; Gerkin, R. M.; Hager, S. L. *J. Elast. Plastic* **1980**, *12*, 184.
(29) Chen, C. H. Y.; Briber, R. M.; Thomas, E. L.; Xu, M.; MacKnight, W. J. *Polymer* **1983**, *24*, 1333.
(30) Xu, M.; MacKnight, W. J.; Chen, C. H. Y.; Thomas, E. L. *Polymer* **1983**, *24*, 1327.
(31) Peebles, L. H., Jr. *Macromolecules* **1976**, *9*, 58.
(32) Assink, R. A. *Macromolecules* **1978**, *11*, 1233.
(33) Assink, R. A. *J. Polym. Sci., Polym. Phys. Ed.* **1977**, *15*, 59.
(34) Assink, R. A.; Wilkes, G. L. *Polym. Eng. Sci.* **1977**, *17*, 606.
(35) Assink, R. A.; Wilkes, G. L. *Polym. Prepr., Am. Chem. Soc., Div. Polym. Chem.* **1977**, *18* (1), 307.
(36) Lagasse, R. R. *J. Appl. Polym. Sci.* **1977**, *21*, 2489.
(37) Froix, M. F.; Pochan, J. M. *J. Polym. Sci., Polym. Phys. Ed.* **1976**, *14*, 1047.
(38) Goldwasser, D. J. *J. Polym. Sci., Polym. Phys. Ed.* **1979**, *17*, 1465.
(39) Spiess, H. W.; Sillescu, H. *J. Magn. Reson.* **1981**, *42*, 381.

Joseph J. Dumais and Lynn W. Jelinski*
AT&T Bell Laboratories
Murray Hill, New Jersey 07974

Louis M. Leung, Irena Gancarz, Adam Galambos, and Jeffrey T. Koberstein
Department of Chemical Engineering
Princeton University
Princeton, New Jersey 08544

Received October 30, 1984

Characterization of Heterogeneous Polymer Blends by Two-Dimensional Proton Spin Diffusion Spectroscopy

Techniques providing information on disorder in solids are of particular importance for the study of synthetic polymers and of biopolymers. The physical properties of polymer blends depend to a large extent on miscibility and on the resulting heterogeneous structure,[1-3] which often results in new interesting mechanical properties of the blends. Disorder has been studied by traditional techniques such as diffraction methods,[4-8] thermal analysis,[9] and electron microscopy.[10] It has also been recognized that spin diffusion in nuclear magnetic resonance can provide information on heterogeneity of polymers.[11-18] Spin diffusion is induced by the dipolar interaction of nuclear spins and leads to a transfer of magnetization between neighboring spins. Because of the $1/r_{ik}^6$ distance dependence of the spin diffusion rate,[19] magnetization transfer is restricted to close neighborhood and delivers information on the spatial proximity of different molecules in a solid.

It is well-known that spin diffusion is of central importance for relaxation in solids by providing relaxation pathways via efficient relaxation centers like paramagnetic inpurities[19,20] and rotating methyl groups.[11-14] Polymeric systems are frequently heterogeneous either with respect to local order (e.g., crystalline and amorphous domains), leading to different mobility of the polymeric chains, or with respect to chemical composition in polymer blends.

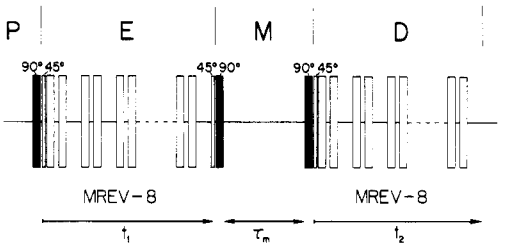

Figure 1. Pulse sequence for 2D proton spin diffusion spectroscopy with magic angle sample spinning. P, preparation by a $\pi/2$ pulse; E, evolution for time t_1 under MREV-8 multiple-pulse decoupling; M, spin diffusion during mixing time τ_m; D, detection in the presence of MREV-8 multiple-pulse decoupling.

In heterogeneous systems, spin diffusion between components in different domains is strongly dependent on domain size, and the measurement of cross-relaxation between different domains provides insight into the domain structure of polymers.[13-15]

In the case that the domains differ in mobility and correspondingly in their transverse relaxation rates, the spin diffusion rate between domains can be measured by the Goldman-Shen experiment[21] or by modified versions of it, including multiple-pulse line-narrowing sequences.[22,23] A more direct approach is possible if the resonance lines of the various components in the domains are spectrally resolved. Then selective polarization transfer experiments can be applied for the measurement of the spin diffusion rate. This is particularly easy for heteronuclear spin systems such as ^1H and ^{19}F[24-26] or for nuclear species with large chemical shift ranges such as ^{13}C. In the latter case, however, isotopic enrichment is necessary to render spin diffusion measurable[27] unless the system has exceptionally slow spin-lattice relaxation so that the spin memory is preserved for a sufficiently long time.[28,29] For practical measurements the techniques of two-dimensional (2D) spectroscopy[30,31] are predestinate. They permit high spectral selectivity and the simultaneous exploration of all cross-relaxation pathways.

In this communication we propose the usage of proton spin diffusion in a two-dimensional (2D) spectroscopy experiment for the study of heterogeneity. Because of the larger gyromagnetic ratio and because of the higher natural abundance, proton spin diffusion is faster than carbon-13 spin diffusion by orders of magnitude. Typical time constants are 100 μs to 10 ms. Even for very short spin-lattice relaxation times, spin diffusion among protons can easily be observed.

A handicap of protons in this application is their small chemical shift range paired with very strong homonuclear dipolar interactions which entirely mask the different chemical shifts. It turns out, however, that by a combination of homonuclear multiple-pulse decoupling and magic angle sample spinning a sufficient resolution can be attained to resolve the relevant chemical shifts in many systems of practical interest.[32-34]

The experimental technique is an extension of the well-known two-dimensional (2D) exchange experiment.[30,31] The pulse scheme is shown in Figure 1. After preparation of transverse magnetization by a $\pi/2$ pulse, the precession in the presence of multiple-pulse decouping labels the magnetization components by their isotropic chemical shifts. A further $\pi/2$ pulse restores longitudinal magnetization which may diffuse in the following mixing time of length τ_m. A third $\pi/2$ pulse is used to monitor the diffusion process. The precessing magnetization, again in the presence of a multiple-pulse sequence, is finally de-

0024-9297/85/2218-0119$01.50/0